International Journal of Plasticity 52 (2014) 117–132

Contents lists available at ScienceDirect

International Journal of Plasticity

journal homepage: www.elsevier.com/locate/ijplas

Stochastic effects in plasticity in small volumes

Shuai Shao [a], Niaz Abdolrahim [a], David F. Bahr [b], Guang Lin [c], Hussein M. Zibib [a,*]

[a] School of Mechanical and Materials Engineering, Washington State University, United States
[b] School of Materials Engineering, Purdue University, United States
[c] Computational Science & Mathematics Division, Pacific Northwest National Laboratory, United States

ARTICLE INFO

Article history:
Received 27 November 2012
Received in final revised form 26 August 2013
Available online 10 October 2013

Keywords:
A. Dislocations
B. Beams and columns
B. Metallic material
C. Probability and statistics
Multiscale

ABSTRACT

Recent studies of micro- and nano-scale metallic structures have exposed considerable statistical distribution, in addition to significant size dependencies, in the yield strength. This intrinsic statistical variation is particularly evident in the micro-compression and micro-tension thin film tests. This work investigates the relationship between the initial dislocation density, the heterogeneous initial spatial dislocation distribution, and the resulting localized deformation with multiscale discrete dislocation dynamics simulations. This relationship is examined separately from commonly reported external factors affecting observed strength, such as variations in specimen geometry and base support. Towards this end, we performed multiscale dislocation dynamics simulations of geometries commonly employed in micro-scale testing techniques, including micro-pillar compression, microtensile thin film, and microbulge tests. The statistical variation of yield strengths from all three simulation geometries is in agreement with experimental data from the corresponding loading techniques. We show that the onset of plasticity is stochastic in small volumes containing a small density of dislocations: a contrast to classical deterministic plasticity theory. The yield stress in these small volumes is stochastic, not deterministic, because of statistical variation of the initial dislocation content. The numerical results exhibit a localized deformation process and demonstrate a strong dependence of the yield stress on the initial dislocation density, the initial dislocation spatial distribution, and the specimen geometry size. Leveraging nucleation theory, a stochastic model for the onset of plasticity in micro- and nano-scale structures is developed based on these results.

© 2013 Elsevier Ltd. All rights reserved.

1. Introduction

Micro scale metallic structures, e.g. micro-pillars and thin films, demonstrate significantly higher yield strengths than their bulk counterparts and exhibit very strong size dependencies accompanied with a jerky deformation process (Uchic et al., 2004; Nix, 1989). This higher strength has been explained by researchers using different theories depending on the various loading techniques. For loading conditions that can impose a strain gradient on specimens, e.g. bending or torque, the size effect can be attributed to geometrically necessary dislocations (GND) (Fleck et al., 1994; Ma and Clarke, 1995; Nix and Gao, 1998; Stolken and Evans, 1998; Zhang and Aifantis, 2011). However, in both experimental and numerical studies, the size dependency of strength has also been observed in macroscopically homogenous loading conditions, e.g. in micro-compression tests (Uchic et al., 2004; Lee and Nix, 2012; Dimiduk et al., 2005; Kiener et al., 2009; Schneider et al. 2011; Tang et al., 2007; Akarapu et al., 2010; Zbib and Akarapu, 2009; Gao et al., 2010; Ng and Ngan, 2008a,b,c; Ngan and Ng, 2010; Zhou, et al., 2010), in thin film microbulge, and microtension tests (Xiang et al., 2006; Yu and Spaepen, 2004; Jaeger et al.,

* Corresponding author.
E-mail address: zbib@wsu.edu (H.M. Zibib).

0749-6419/$ - see front matter © 2013 Elsevier Ltd. All rights reserved.
http://dx.doi.org/10.1016/j.ijplas.2013.09.005

2006; Hommel and Kraft, 2001; Nix, 1989; Gruber et al., 2008; Huang and Spaepen, 2000). The theory of GND is not applicable in these cases because of the absence of macroscopic strain gradients. Rather the high strength and size dependence can be attributed to the scarcity of dislocations in small volumes, and the strong interactions of dislocations with obstacles and surfaces (Rhee et al., 1994; Uchic et al., 2004; Akarapu et al., 2010; Zbib and Akarapu, 2009; El-Awady et al., 2011). The size effect on the strength of micro-pillars and thin films has been studied quite extensively over the past few years (Lee and Nix, 2012; Akarapu et al., 2010; Zbib and Akarapu, 2009; Hommel and Kraft, 2001; Nix, 1989; Gruber et al., 2008; Brotzen, 1994; El-Wady et al., 2011), and different scaling models for the size effects have been proposed. The compressive strength of micro-pillars generally decreases as a power law with increasing pillar diameter (Lee and Nix, 2012):

$$\tau_{CRSS} = \tau_0 + A \cdot D^{-n} \tag{1}$$

where τ_{CRSS} is critical resolved shear stress required to activate a dislocation arm in micro-pillars, τ_0 is the shear strength in bulk material, D is the diameter, and A and n are model parameters. Commonly thin films are polycrystalline materials, so the presence of grain boundaries also affects the thin film strength (Lawrence et al., 2012). Therefore, the tensile strength for thin films is more complex and depends on both the film thickness and grain size (Hommel and Kraft, 2001; Nix, 1989). However many investigators have also shown that the strength-thickness relationship in a thin film geometry follows Eq. (1) (Gruber et al., 2008; Brotzen, 1994).

In the literature, modeling of the size effect in microscale metallic structures treated the onset of plasticity as a deterministic event. In striking contrast to this assumption is the large amount of microscale experimental data: the data display a significant amount of statistical variation and a jerky flow process regardless of how careful and elegantly the experiments are performed (Dimiduk et al., 2005; Kiener et al., 2009; Schneider et al., 2011; Yu and Spaepen, 2004; Jaeger et al., 2006; Hommel and Kraft, 2001; Gruber et al., 2008; Huang and Spaepen, 2000; Rinaldi et al., 2012; Lawrence et al., 2012; Li et al., 2012). For instance, Kiener et al. (2009) have observed a variation of about 200 MPa (maximum difference) in the yield shear strength corresponding to micro-pillars with diameters under 1 micron. In other experimental work, including micro-compression tests, microbulge tests, and microtension tests on various FCC and BCC materials, a conspicuous amount of variation is present in the data. The cause of this significant variation was largely categorized into the similar systematic errors as listed by Kiener et al. (2009) and Kraft et al. (2010). These studies suggest the strength in metals at small length scales is strongly dependent on the underlying dislocation mechanisms: how dislocations interact with grain boundaries, interfaces, and various defects which may be present in the crystal. The size effect on small scale metal strength can be addressed rigorously by means of discrete dislocation dynamics (DD).

The DD method is suited for tackling problems where size effects and interfaces are important for two reasons: First the constitutive behavior of a small material volume is captured naturally within the DD simulations, reflecting the effect of both the microstructure and the internal/external geometry of the material e.g., Groh et al. (2009); Second the dynamics of an individual dislocation can be sensitive to any changes in the scale describing the problem, and these changes are directly determined in DD. For example, Deshpande et al. (2005), Benzerga and Shaver (2006), Guruprasad and Benzerga (2008) have performed two dimensional (2D) dislocation dynamics simulations on a planar single crystal both under tension and compression. These studies examined the underlying dislocation mechanisms responsible for the macroscopic response of micro-pillars. Although the 2D dislocation analyses provided useful insights, these analyses lack many key three dimensional (3D) dislocation interactions. 3D-DD analyses of micro-pillars have been performed by an number of investigators. For example, the works of Tang et al. (2007, 2008), Rao et al. (2008), Zbib and Akarapu (2009), El-Awady et al. (2009), Zhou et al. (2010), and El-Awady et al. (2011) show that 3D-DD can capture the dependence of the yield stress on the specimen size, initial dislocation density, and loading conditions. Furthermore through the use of 3D-DD analyses, the large statistical variation in the flow stress was attributed to several factors: loading direction (Zhou et al., 2010), initial dislocation content and boundary conditions (Zbib and Akarapu, 2009; El-Alwady et al., 2009), and density pre-straining (Schneider et al., 2013; El-Awady et al., 2013).

In order to investigate the plastic deformation in finite sizes such as in the cases of micro-pillars and thin films, the conventional dislocation dynamics framework needs to account for surface effects and heterogeneous deformation fields. Experiments show that the deformation field in micro-pillars and thin specimens is heterogeneous and becomes highly localized with increased strain. Yasin et al. (2001) coupled 3D-DD with the finite element method and showed that surface effects cannot be ignored regardless of size, and may result in errors as much as 10%. Akarapu et al. (2010) showed that slip bands with local strains approaching 50% occur in micro-pillars, highlighting the extreme heterogeneity in the strain fields.

Surface effects within the DD framework have been addressed by a number of investigators using the concept of image stresses when dislocations are in finite volumes, while heterogeneous deformation is addressed by coupling DD with continuum plasticity (see a recent review article by Groh and Zbib, 2009). Generally, the solution to the surface effects in DD is based on the superposition method proposed by Van der Giessen and Needleman (1995). The solution is obtained as the sum of two contributions. The first represents the solution for dislocations in an unbounded crystal and the other is the complementary elastic solution needed to satisfy equilibrium at external and internal boundaries. The second solution can be solved in a continuum mechanics way, such as finite element methods, see for example, Van der Giessen and Needleman (1995), Yasin et al. (2001), Martinez and Ghoniem (2002), Zbib and de la Rubia (2002), or the boundary element method, see, for example Fivel et al. (1996) and El-Awady et al. (2008). Khraishi and Zbib (2002) developed a rigorous method to handle the issue of image stresses. The method is semi-analytical/numerical in which they enforce either traction or

displacement boundary conditions at collocation points on a surface. In addition to the issues of surfaces and image forces, the multiscale model developed by Zbib and de la Rubia (2002) integrates dislocation dynamics with continuum plasticity in such a way that the dislocation dynamics replaces the macroscopic constitutive equation, making it possible to address complex boundary value problems and to capture the heterogeneity of the macroscopic deformation and stress fields.

In this paper we use the method developed by Zbib and de la Rubia (2002) to analyze the observed plasticity in small volumes with focus on micro-pillars and thin films. We suggest that the major contributor to the uncertainty in the initial yield stress is related to the initial condition of the dislocation content: the initial dislocation density and the initial dislocation spatial distribution. For example, micro-pillars are normally fabricated using focused ion beam machining from a larger structure, either a film or bulk crystal. A fabricated micro-pillar may have a higher or lower dislocation density depending on the local property of the base material from where it is "machined." Even if the dislocation densities of two micro-pillars are the same, the distribution of the dislocations can greatly differ between the two: the dislocations can be rather concentrated in a portion of one micro-pillar and evenly spread across the other. Such differences in the initial dislocation content among the micro-pillars can seriously affect the plastic deformation, leading to different levels of yield stresses for two pillars with identical geometries. This conundrum has been suggested before by other researchers (Ng and Ngan., 2008a,b,c; Rinaldi et al., 2012; El-Awady et al., 2009, 2011; Zhou et al., 2010; Guruprasad and Benzerga., 2008). A similar situation is observed in thin films. The distribution of the dislocation network in thin films differs between different substrates and varies among areas on the same substrate. Depending on where a testing window is etched for a bulge test, the yield stress value could be different. Bulge tests often sample lateral dimensions on the order of millimeters with sub-micron thicknesses, but micro-pillars often sample lateral dimensions on the order of microns. It has been reported that the observed statistical variation of yield stress for micro-pillars is significantly more pronounced than the variation in thin films (Akarapu et al., 2010; Zbib and Akarapu, 2009). As shown in those studies, the primary deformation mechanism of micro-pillars under compression is the spiral motion of dislocations. This mechanism tends to "contain" the deformation in a small region followed by strain bursts. Due to this confining deformation mechanism, the yield strength measured in micro-pillar geometries is very sensitive to the initial distribution of dislocations. As a result, data sets of strength values with a relatively large standard variation corresponding to a single micro-pillar size are common. On the other hand, the dislocations in the thin films tend to be laid out in an across-the-thickness manner, and the deformation is governed by the threading motion of the dislocations. This threading mechanism tends to distribute the deformation field through a wider area; therefore, the yield strength measured in thin film geometries is less sensitive to the initial dislocation density (e.g., density, concentration, etc.).

The deformation process in micron and sub-micron scale specimens has been shown to occur in sequences of strain burst resulting from locking/unlocking dislocation mechanisms (pile up stress concentration regions and or formation and break-up of junctions). Ng and Ngan (2008a,b,c), Ngan and Ng (2010) and Zaiser et al. (2010) viewed the jerky flow deformation process as stochastic events within a statistical theory. The jerky flow phenomenon was investigated by Hiratani and Zbib (2002, 2003) using stochastic discrete dynamics, where the dislocation motion was viewed within the framework of stochastic Brownian dynamics. The aim of the present work is to develop a thorough understanding of the behavior of the yield stress in the small-volume metallic structures, with respect to the change of the length scales, using discrete dislocation dynamics DD coupled with continuum finite element analyses. We employ dislocation dynamics to investigate the jerky and localized flow phenomena encountered during three of the most popular micro-testing techniques: microcompression tests, micro-bulge tests, and microtension tests (Uchic et al., 2004; Brotzen, 1994; Gianola and Eberl, 2009). DD simulation models of micro-pillar and thin film geometries under such loading conditions were constructed and tested. To mimic realistic experimental situations and reproduce the statistical variation in the data, the initial density and distribution of the dislocations are varied in a controlled manner. The results are collected, compared to the experimental data, and then analyzed to enable a fuller understanding of the stochastic effects in the onset of plasticity in microstructures. The size effect is observed, and rigorous statistical analyses incorporating the nucleation theory are performed. Our approach is to treat the event of onset of plasticity in small volumes as a "stress relaxation event," and, to this end, we introduce the nucleation theory to describe plastic onset. In general, the rate of a stress relaxation event $\dot{N}$ that is produced by any thermally-activated inelastic mechanism can be expressed as (Kobrinsky and Thompson, 2000)

$$\dot{N} = \mathrm{N}\upsilon_D exp\left(\frac{-\mathrm{Q}(\overline{\sigma},\mathrm{T})}{\mathrm{k_B T}}\right) \tag{2}$$

$$\mathrm{Q} = \mathrm{Q}^* - \sigma \mathrm{v}^*$$

where N is the number of equivalent nucleation sites, υ_D is Debye frequency, k_BT is the thermal energy, Q is the activation free energy which is a function of temperature and stress, and Q^* is the activation enthalpy. Activation volume is the rate of activation free energy with respect to the flow stress at constant temperature: $\upsilon^*(\overline{\sigma},T) \equiv -\frac{\partial Q}{\partial \sigma}\big|_T \approx k_BT\frac{\partial \ln(N)}{\partial \sigma}$ (Zhu et al., 2008). This quantity can be defined as the volume or the number of dislocations contributed in an activated process. Therefore activation volume can be considered a kinetic signature of the deformation mechanism. For competing processes with the same activation energy (which is the case in this work, as will be shown later), the activation volume is a good measure for determining the operative deformation mechanism because it characterizes the rate dependency of the activation energy on the stress. Schuh and Lund (2004) have suggested a relation between $\dot{N}$ and the cumulative fraction function, which in turn

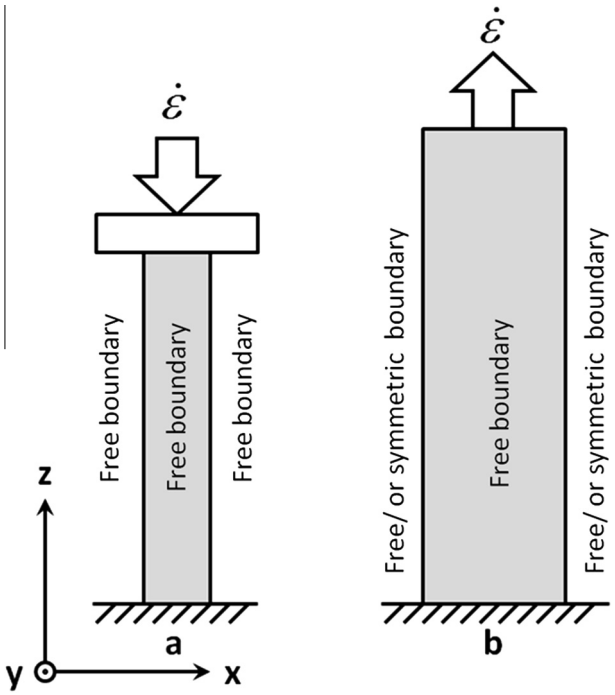

Fig. 1. Boundary conditions applied to the DD simulations.

is the derivative of the probability density function (PDF). A model predicting the PDF of the onset of plasticity at a given yield stress in a microstructure at a given length scale can therefore be constructed. Here we adopt the same method and use the results from both experiments and discrete dislocation dynamics DD simulations coupled with continuum finite element analyses to determine the model parameters and the dependence of these parameters on the dislocation density.

2. Computational details

In this work we employ a hybrid model developed by Zbib and Diaz de la Rubia (2002), which combines microscopic mechanisms and dislocation dynamics with the macroscopic deformation of the solid. The model couples a stochastic discrete dislocation dynamics model with a continuum elasto-visoplasticity model, using the principle of superposition in addition to the finite element formulation to satisfy boundary conditions. The coupling is based on a framework in which the material obeys the basic laws of continuum mechanics. The result is a hybrid multiscale model termed *a "multiscale dislocation dynamics plasticity – MDDP*" possessing the following two main features[1]: (1) Coupling of the continuum mechanics problem with discrete dislocation dynamics, and (2) an ability to robustly deal with multiple possible boundary conditions, interfaces, and dislocations in heterogeneous materials. The details of the MDDP multiscale model have been discussed in detail in previous papers, particularly in Zbib and de la Rubia (2002), Hiratani and Zbib (2002), Groh et al. (2009), Zbib et al. (2011).

We performed several MDDP simulations of the experimental techniques of interest: the micro-pillar compression test, the microbulge test, the microtension test, on Cu micro-pillars and thin films. The boundary conditions applied to the simulations are demonstrated in Fig. 1. For all the cases, one end in z direction is fixed while the other end is subjected to a displacement with a constant strain rate $\dot{\varepsilon} = \pm 100\, s^{-1}$. For the micro-pillars, all other surfaces are left traction free and the strain rate $\dot{\varepsilon}$ is negative, to best simulate the micro compression test. In the thin films microtension test, all lateral surfaces are left traction free, and the strain rate $\dot{\varepsilon}$ is positive. In the bulge test case, a symmetric boundary condition is applied to both ends in x direction. Further details on treatment of boundary conditions can be found in Akarapu et al. (2010). The size of the models ranges from 200 nm to 1000 nm in diameter for the micro-pillars, and from 160 nm to 2400 nm in thickness for the thin films. The aspect ratio of the micro-pillars is $1 \times 1 \times 5$ and $1 \times 5 \times 10$ ($x \times y \times z$) for the micro-pillars and thin films respectively.

The material properties used in the simulation are summarized in Table 1. The values for the dislocation mobility and stacking fault energy, and the effect of these variables on the DD prediction have been addressed in a number of articles, e.g. Kubin et al. (1992), Rhee et al. (1998) and Zbib et al. (1998). In the compression experiments of single crystal Ni micro-pillars, Shan et al. (2008) observed an initial high dislocation density of the order of $\sim 10^{15}$ ($1/m^2$). This density is almost

[1] More details about the *micro3d* and *MDDP* software can be found at www.cmm.wsu.edu

Table 1
Material and control parameters of the MDDP simulations.

Material and control parameters	Value
Density (kg/m^3)	8960
Shear modulus (Pa)	4.83e+10
Poisson's ratio	0.3
Dislocation mobility (1/Pa sec)	1000
Burgers vector magnitude (m)	2.5e−10
Temperature (K)	300
Staking Fault Energy (J/m^2)	0.04

three orders of magnitude larger than the typical density for a well annealed material in bulk ($\sim 10^{12}$/m^2). Shan et al. (2008) also classified the defects into two types of dislocation sources: small loop-like, and long arm like. Additionally Kiener et al. (2008) argued that the partial removal of initial dislocation sources during FIB milling produces single dislocation arms. Based on these experimental observation and suggestions, Akarapu et al. (2010) used dislocation arms and Frank-Read sources as models for dislocations in micro-pillars and thin films. Similar observations and models for dislocation sources in micro-pillars have been proposed by other investigators, e.g. Espinosa et al. (2006); Tang et al. (2007, 2008), who also noted initial dislocation densities ranging from 10^{13} to 10^{14}/m^2. In the present work, several initial dislocation densities ρ have been tested, ranging between 1.0 and 100 μm^{-2} for the micro-pillars, and from 3 μm^{-2} to 10 μm^{-2} for the thin films. Various spatial and initial distributions of existing Frank-Read sources and jogged dislocation arms extending from one surface to the opposite surface are considered. During the simulations, dislocations segments may cross-slip, generating new sources. This mechanism has been discussed by Akarapu et al. (2010), where a clear correlation among the dislocation bursts, the stress drops, the formation of junctions, and the activation of cross-slip is shown. Furthermore, it is shown that during the burst process, the dislocations that cross-slip and glide to the surface, and as these dislocations terminate at the surface they cause distortion, resulting stress concentrations. Homogenous nucleation and nucleation of new sources from surfaces is not considered in this work. However, nucleation criteria can be introduced by establishing a criterion nucleation (see e.g. Shehadeh et al., 2006). Here we introduce only initial dislocation sources; for smaller micro-pillars with low ρ_{disl} a macroscopic yield point is not observable due to the scarceness of dislocations. In contrast, for larger pillars and thin film models with high $\rho_{\text{disl.}}$, the computation becomes prohibitively expensive. For these reasons, in the extreme cases of $\rho_{\text{disl.}}$, the complete size range is not covered. For each density-size combination, five different spatial distributions of dislocations are considered, representing cases of homogenous and heterogeneous distributions (Fig. 2). Outside of the case of evenly distributed dislocations, the other cases limit the dislocations to 1/2, 1/3, 1/4 and 1/5 of the sample length in z direction. In this way the local dislocation density has been multiplied by factor of 2, 3, 4 or 5, respectively. Fig. 3 shows samples of the various initial dislocation networks created via the manipulations mentioned above, i.e. different density and distribution of dislocations. The crystallographic orientation considered in this work is [100]//x, [010]//y, [001]//z.

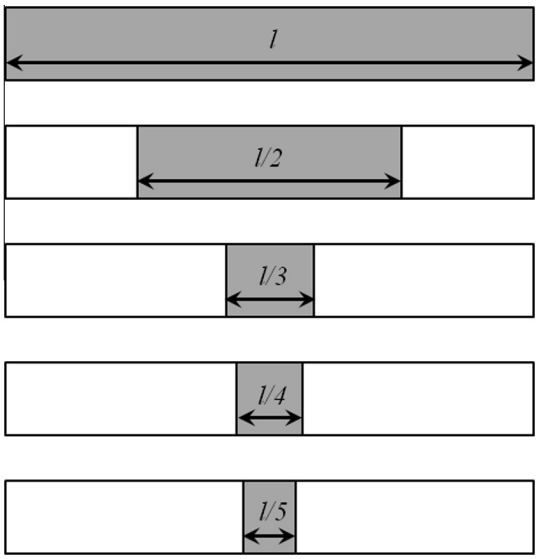

Fig. 2. The initial dislocations' distribution is limited spatially in the loading (z) direction.

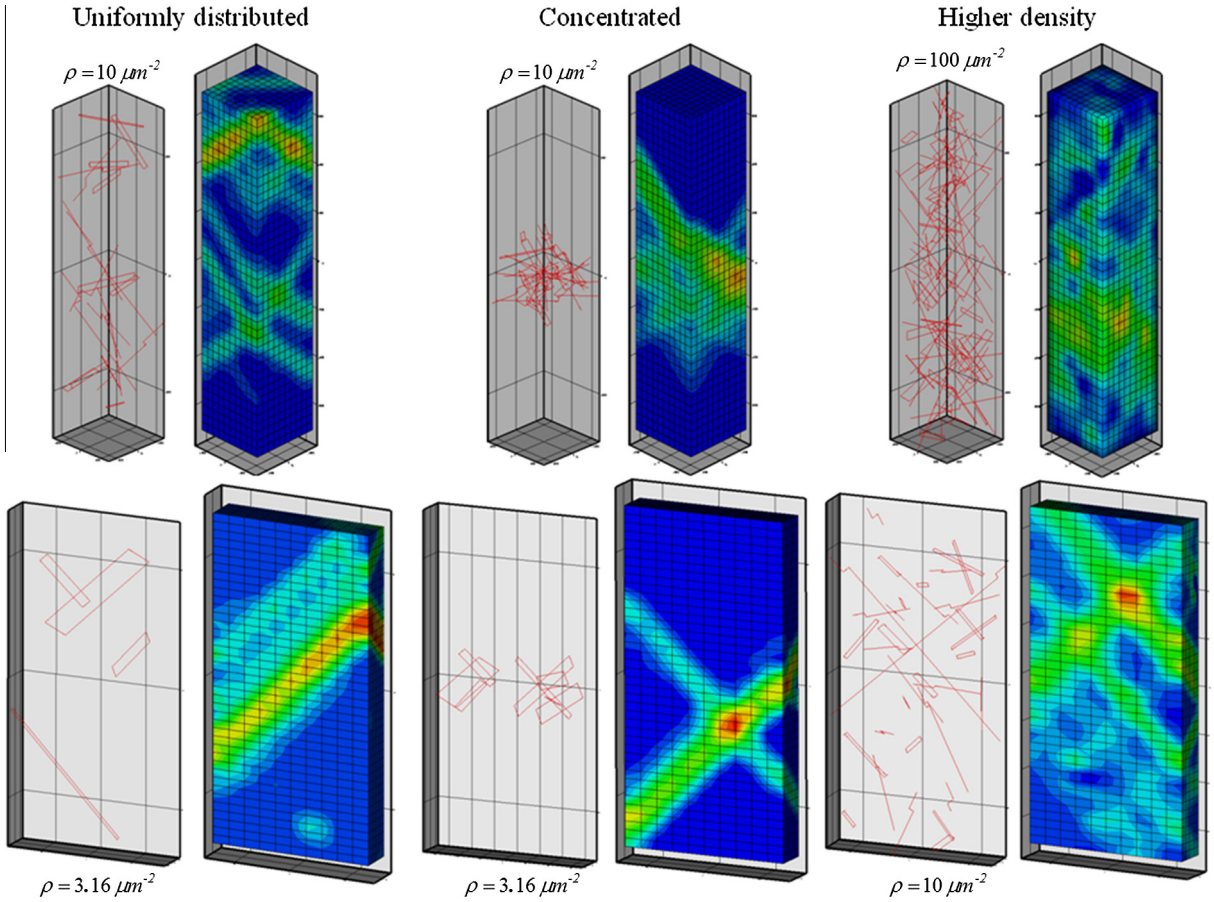

Fig. 3. Illustration of the different initial configurations of dislocation networks in DD and the resulting deformation field (colored according to normal plastic strain in *z*/vertical direction).

3. Results and analyses

The resulting stress strain curves from all the simulations are shown in Figs. 4 and 5. Each graph displayed Fig. 4a–e contains only curves corresponding to micro-pillars of the same size. In Fig. 5a–d, the curves for the thin films with the same size have been coded in similar colors in each graph. We note the wide spread of the data from structures with the same dimensions in these curves, and we remark on the data spread caused solely by the initial conditions of the dislocation networks. The normal plastic strain field plots in Fig. 3, for a few studied cases, show that the deformation of the metallic structures was indeed significantly affected by the initial configuration of dislocation networks. To better illustrate the data spread, the yield point of each curve has been extracted by taking a 0.1% and 0.05% offset for the micro-pillars and for the thin films respectively. In the following subsections, the yield data for the micro-pillars and the thin films are analyzed in detail. In passing we note, that although the focus of this paper is the yield stress and its dependence on size and initial dislocation density, our results also show that the hardening rates increase with decreasing size and initial dislocation density. Further analyzes are needed to better quantify this effect on hardening, and these analyzes are left for future studies.

3.1. Analyses of the yield strengths of the micro-pillars – a probabilistic model

The yield stress data, from micro-pillars corresponding to the 0.1% offset, are summarized in Fig. 6. It is evident that, collectively, the yield stress and the extent of variation in the yield stress σ_y decrease with increasing initial dislocation density ρ. On average the stress decreases with increasing specimen size. We note an exception is at $\rho = 1.0\ \mu m^{-2}$ where the span of data is much smaller compared to higher density entries. In Fig. 6 each group is coded using the same color. The data shown in Fig. 6 can be fitted to a power law $\sigma_y \propto \rho^{-m}$. Except for the 200 nm case, m is almost consistently equal to 0.36 ± 2; for the 200 nm case m = 0.54. Recent DD results by El-Awady et al. (2013) yielded m = 0.18. The larger m value for the 200 nm case can be attributed to the scarcity of dislocations, and as the density decreases the dislocations become even scarcer.

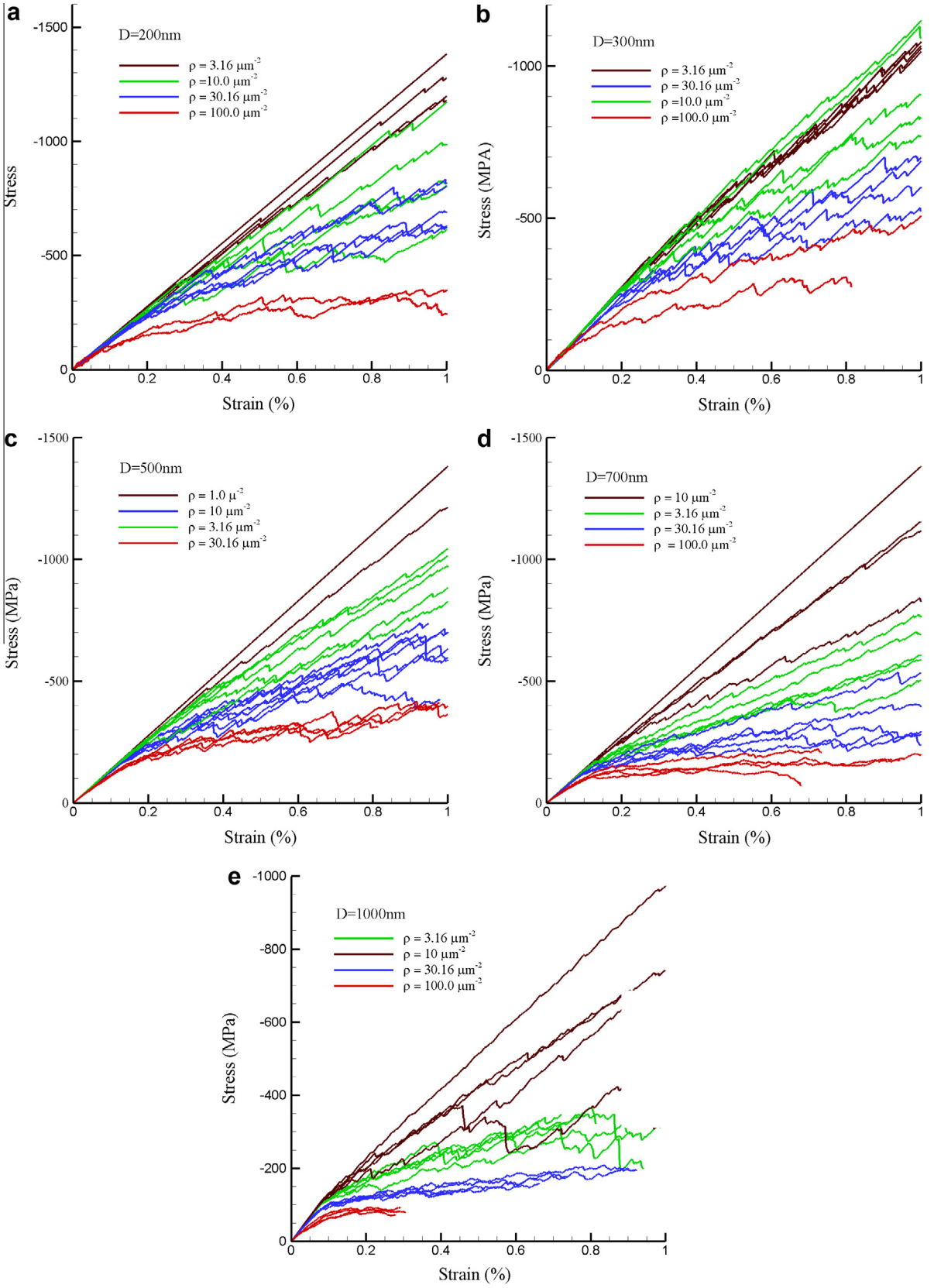

Fig. 4. The stress strain curves of MDDP simulations of micro-compression tests on micro-pillars.

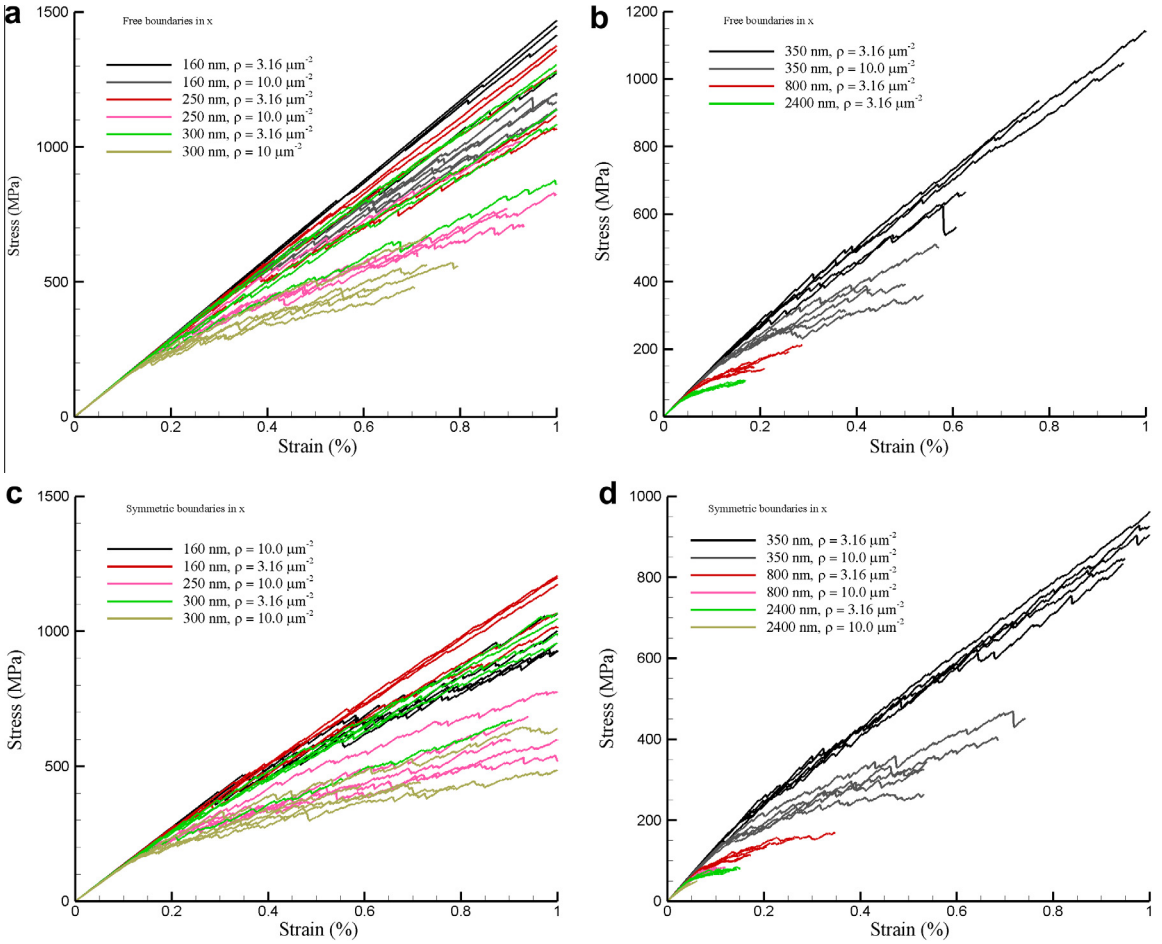

Fig. 5. The stress strain curves of MDDP simulations of microtension tests (free boundaries in x) and micro-bulge tests (symmetric boundaries in x) on thin films.

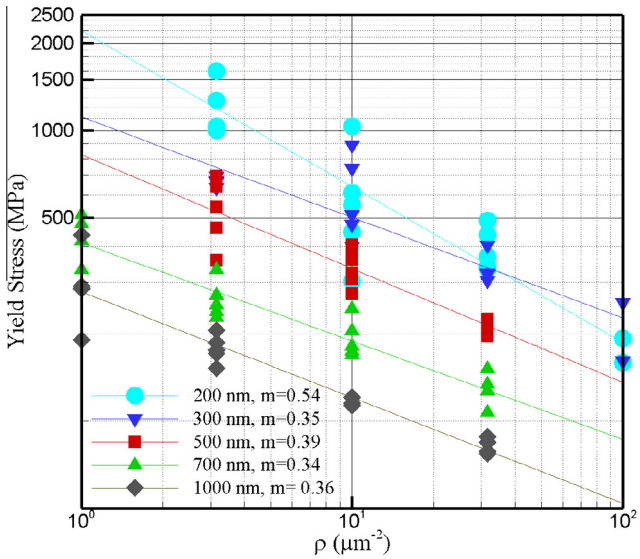

Fig. 6. The variation of yield strength (0.1% offset) with respect to the square root of the initial dislocation density.

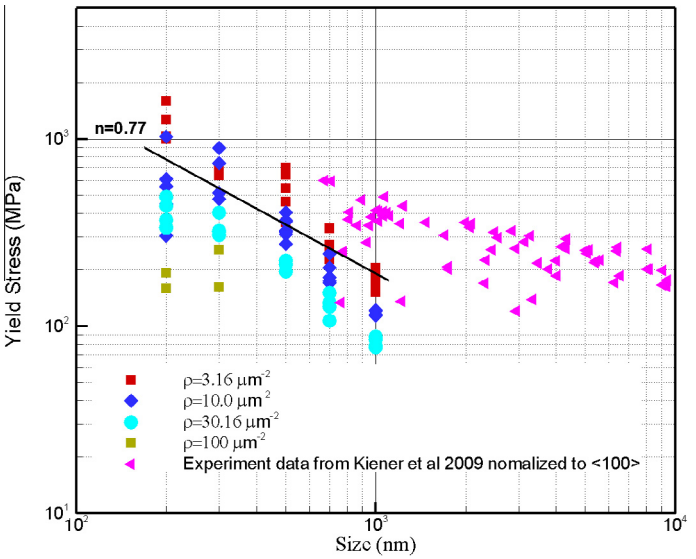

Fig. 7. The variation of yield strength (0.1% offset) with respect to the change in length scale, simulation data, and experiments.

The yield strength and its statistical distribution also decrease with increasing diameter of the micro-pillars (Fig. 7). Again this trend is consistent throughout each dislocation density group. The smaller spread of data in higher dislocation densities and larger specimen sizes is due to the larger population of dislocations in such conditions. As shown by Akarapu et al. (2010); Zbib and Akarapu (2009), the plastic deformation is governed by the operation of spiral dislocation sources. The stagnation and movement of the dislocation arms cause the hardening and bursts of load drop (serrations) in the plastic portion of the stress strain curves. The more abundant the operable dislocations are, as in larger micro-pillars and in pillars with higher dislocation density, the smaller the serrations will be; therefore the grouping of the stress strain curves tend to be tighter in the higher dislocation density cases. On the other hand, when fewer dislocations are present, the serration becomes more severe; resulting in further spread apart of yield strength data. A comparison with the experimental data indicates the reliability of our simulations. Kiener et al. (2009) have performed micro-compression tests on various single crystal Cu micro-pillars. This study involved different orientations, cross-sections shapes, top layers, and aspect ratios of micro-pillars. The corresponding Schmid factors have been applied to the data to normalize it to compression stress in the (100) orientation. We combined our simulation data with the experimental data from Kiener et al. in Fig. 7. From this figure we note that the two sets of data are in good agreement. The discrepancy among the data sets for diameter sizes near 1000 nm results from the different methods used to determine the yield stress: the experimental data is taken at 10% strain (no offset is performed) while we used a lower 0.1% strain offset. Fig. 7 also shows that the degree of data spread between the two sets of data is in good agreement. The experimental data also demonstrate a clear decrease of the variation in yield strength as the size increases; finally the extent of data spread present in both data sets is similar when the two data sets overlap. The numerical result shown in Fig. 7 can be fitted to a power law (Eq. (1)) with $n = 0.77$. This value is in close agreement with a wide range of experimental observations, e.g. Frick et al. (2008); Kraft et al. (2010), and is close to the numerical results value reported in El-Awady et al. (2009).

Next we utilize the concept of percent uncertainty to measure the extent of data spread with respect to the mean value of a quantity: in this case the mean value of yield strength for micro-pillars of a given size. The percent uncertainty can be defined as

$$U_p = \frac{s_\sigma}{\overline{\sigma}}, \quad \text{and} \quad s_\sigma = \sqrt{\frac{\sum_{i=1}^{N}(\sigma_i - \overline{\sigma})^2}{(N-1)}} \tag{3}$$

where s_σ is the standard deviation, and $\overline{\sigma}$ is the mean yield strength. The percent uncertainty of the data of our simulations on micro-pillars and the experiment data are plotted and compared in Fig. 8. The experimental data was grouped by micro-pillar size prior to the calculation the standard deviation. The horizontal error bar denotes the deviation of the sizes in each group. Fig. 8 clearly shows that the DD results are in general agreement with the experiments. As shown the percent uncertainty decreases as a power law as the size (diameter) of the micro-pillar increases, i.e. $U_p \propto 1/s^{0.38}$.

The percent uncertainty is capable of describing the statistical distribution of the existing strengths values. However, the percent uncertainty does not contain any information regarding the actual mean values of the strength, nor can it predict the stochastic yield behavior of micro-pillars at a given size. To overcome these limitations, we use a well-defined PDF which can generate probability values of a given yield stress for a micro-pillar at a given size. Considering that the PDF is the derivative of the cumulative fraction function (CDF), $P = F'_\sigma$, the current simulation data, summarized in Fig. 7, is first converted into

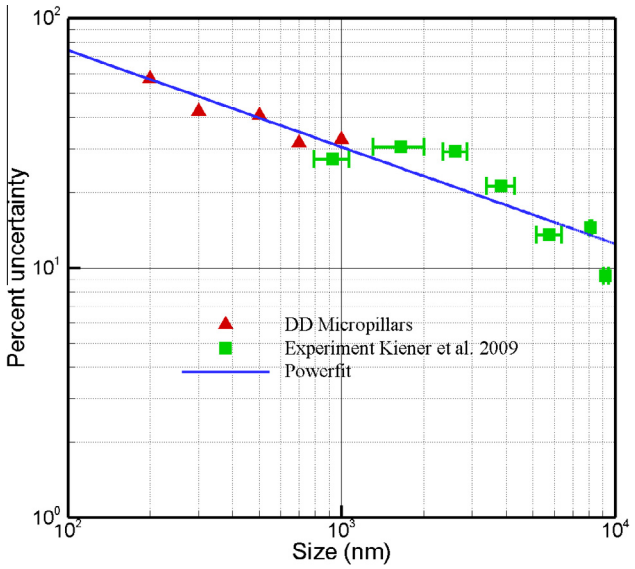

Fig. 8. The variation of percent uncertainty of yield strength of micro-pillars with respect to the change in size (diameter).

cumulative fraction graphs, shown in Fig. 9. We observe from this figure that the curves become steeper as the size (diameter) becomes larger, indicating a smaller extent of variation in the strength data. In this work, we maintain a constant strain rate of $\dot{\varepsilon} = -100\ s^{-1}$. Since we are interested in the onset of plasticity, we employ the reasonable assumption that the loading rate before yield is also constant: $\sigma = \dot{\sigma} \cdot t$. The derivative of F with respect to stress σ is therefore related to the derivative of F with respect to time t as

$$\frac{dF}{dt} = \dot{\sigma}\frac{dF}{d\sigma} = \dot{\sigma}P \tag{4}$$

As suggested by Schuh and Lund (2004), the rate of change of cumulative fraction F is written as

$$\dot{F} = (1 - F) \cdot \dot{N} \tag{5}$$

where $\dot{N}$ is the activation rate (Kobrinsky and Thompson, 2000; Zhu et al., 2008; Schuh and Lund, 2004; Mason et al., 2006) of the event: "onset of plasticity",

$$\dot{N} = N_o \cdot e^{-\frac{Q^* - \sigma v^*}{kT}} \tag{6}$$

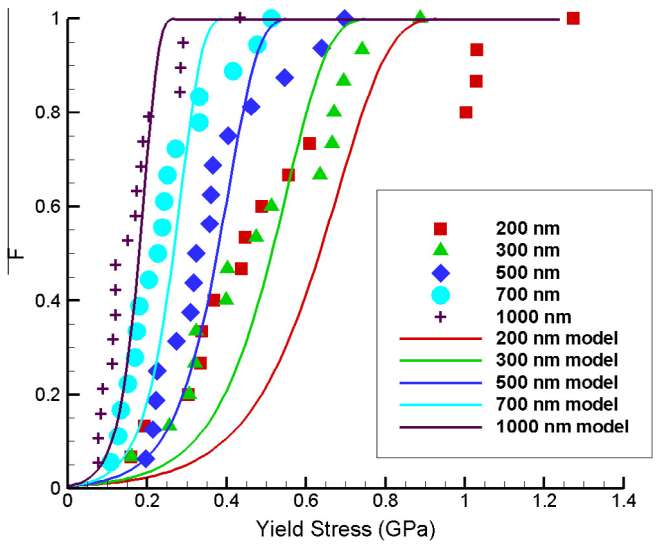

Fig. 9. The cumulative fraction plots of the yield strengths of micro-pillars of varying sizes subjected to compressive loading.

N_0 is the attempt frequency, Q^* is the activation enthalpy, υ^* is the activation volume, k and T are the Boltzmann's constant and absolute temperature. Activation volume is the rate of activation enthalpy with respect to the flow stress at constant temperature. It can be defined as the volume or the number of dislocations contributed in a thermally activated process; therefore, the activation volume can be defined as a kinetic signature of the deformation mechanisms. For competing processes with the same activation energy, the activation volume is a good measure to determine the operative deformation mechanism, because activation volume characterizes the rate dependency of the activation energy to the stress.

If each yielding event is treated as a one-time event and Eq. (4) is substituted into Eq. (5), the probability of the next yield event is proportional to the amount of samples left and the activation rate $\dot{N}$. Integrating Eq. (5) over time on both sides yields (Schuh and Lund, 2004)

$$F = 1 - \exp\left(-\frac{N_0 kT}{\dot{\sigma}\upsilon^*} \cdot \exp\left(\frac{\sigma\upsilon^* - Q^*}{kT}\right)\right) \tag{7}$$

Eq. (7) can be fitted to the data points in Fig. 9. To ensure that the probability of the onset of plasticity is sufficiently small, a boundary condition $f(0) = \delta$ is also enforced, where δ is a very small number: $\delta = 0.05$ is used in this work. The model shown in Eq. (7) is based on the experimental data and numerical results, and this equation works well with all the diameters except for 200 nm. For the larger specimens, the deformation is dominated by the activation of the dislocation sources. Conversely, when the specimen is small, the deformation should be controlled by the nucleation of new dislocation sources. The fact that the nucleation of dislocations is not considered in the MDDP simulations should be the cause of the deviation between the model and the data. Similar observations and reasoning are made for the fittings for the thin film data, as will be shown later.

The fitting parameters are summarized in Fig. 10. The activation volume increases linearly as the diameter of the micro-pillars increases (Fig. 10a). The activation volume is also interpreted as the volume of the dislocation lines which have swept through during the activation process. For that reason, when the diameter approaches zero, the activation volume should

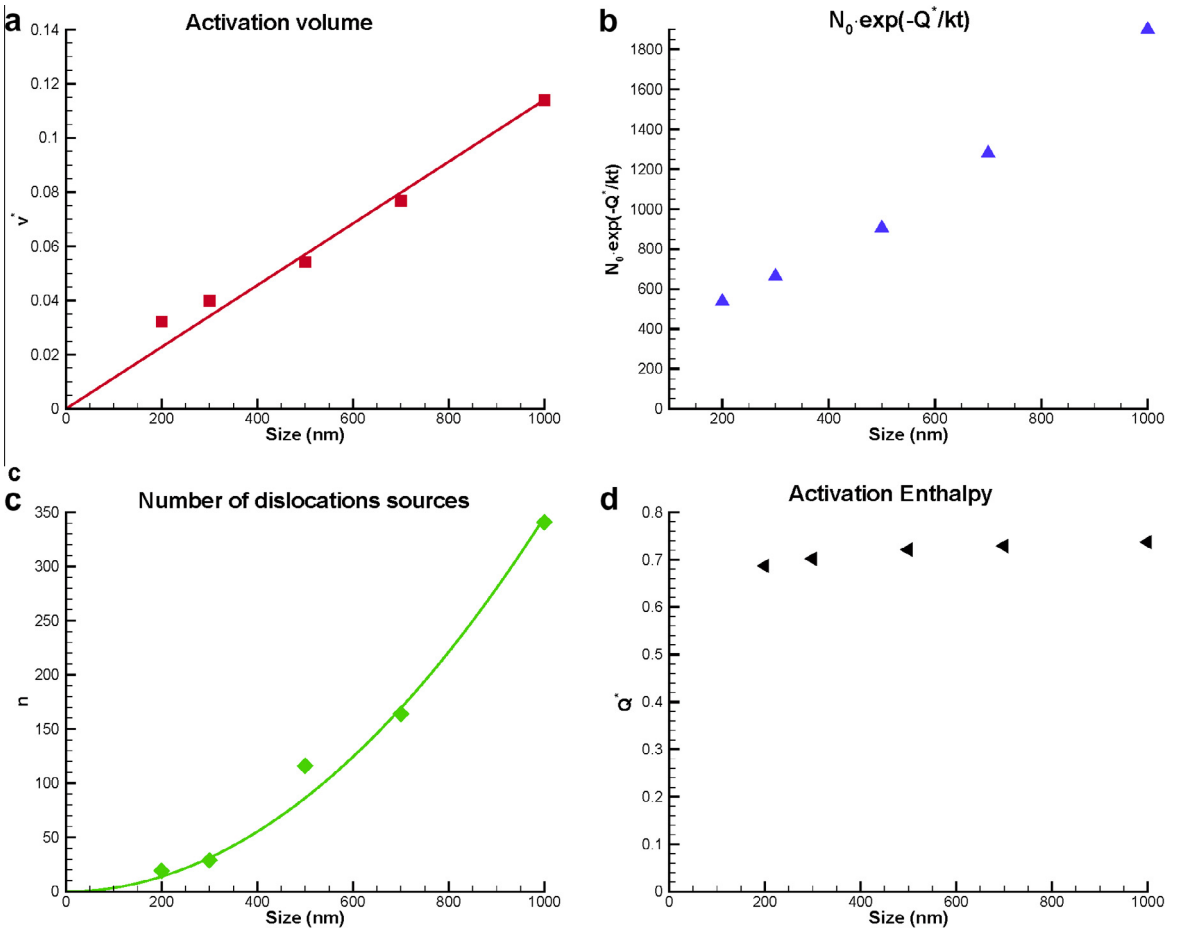

Fig. 10. The plots of (a) activation volume, (b) N_o.exp (- Q^*/kt), (c) nominal number of sources, and (d) activation enthalpy with respect to the change of size (diameter) for the micro-pillars.

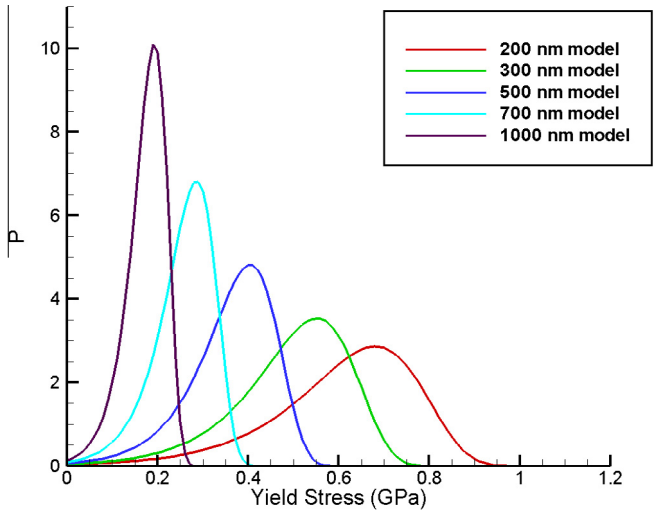

Fig. 11. The resulting probability density functions for the micro-pillars.

also approach zero. We therefore assume $\upsilon^* = \alpha s$, where $\alpha = 1.14 \times 10^{-4}$ nm^2. Fig. 10b shows the variation of $N_o \cdot \exp(-Q^*/kt)$ with the size (diameter) of micro-pillars. Here, two undetermined parameters are in play: the N_o and Q^*. To determine activation enthalpy, we first define N_o. The attempt frequency N_o can be decomposed as, $N_o = n \cdot \upsilon_D$, where n is the nominal number of sources and the latter is the Debye frequency. Furthermore n can be calculated as $n = V\rho_{disl}/l$, where V is the volume of the micro-pillars, $\rho_{disl.}$ is the nominal dislocation density, and l is a characteristic dislocation source length. An average dislocation density of $1 \times 10^{13.5}$ is used. This calculation essentially divides the total length of dislocations by a representative source length. Assuming the source lengths change with the size of the micro-pillars, n is simplified as $n = \beta s^2 \rho = \beta(s/l^*)^2$, where $l^* = 1/\sqrt{\rho_{disl}}$ is the mean free path of the dislocation, with $\beta = 10.95$ (Fig. 10c). In this way, N_o is determined, and Q^* can be calculated (Fig. 10d). The activation enthalpy is roughly constant at for micro-pillars Q^*=0.72 eV.

As a result the fully defined cumulative fraction PDF is written as

$$P = \frac{N_0}{\dot{\sigma}} \cdot \exp\left[\frac{\sigma\upsilon^*}{kT} - \frac{Q^*}{kT} - \frac{N_0 kT}{\dot{\sigma}\upsilon^*} \cdot \exp\left(\frac{\sigma\upsilon^*}{kT} - \frac{Q^*}{kT}\right)\right] \tag{8}$$

where $\upsilon^* = \alpha s$ and $N_0 = \beta\upsilon_D(s/l^*)^2$.

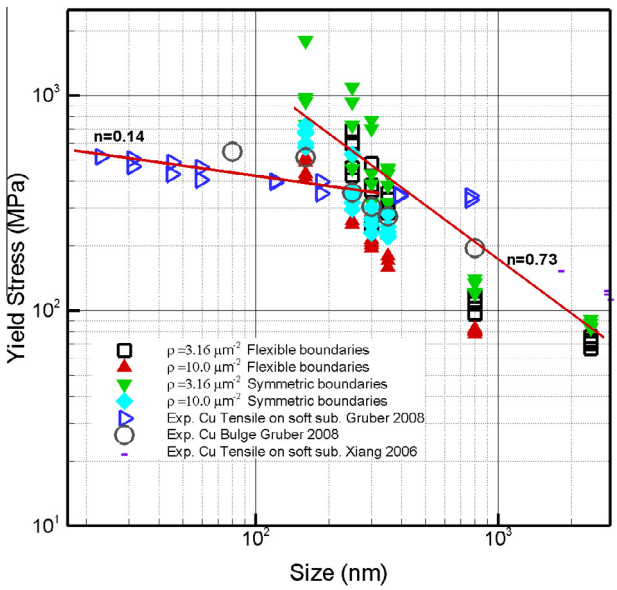

Fig. 12. The yield strengths (0.05% offset) of the thin films with different boundary conditions.

The fitted cumulative fraction data and the resulting PDFs are plotted in Figs. 9 and 11. The PDF changes from wider and lower peaks corresponding to smaller micro-pillar diameters to higher and narrower peaks corresponding to larger diameters. This trend confirms that the extent of statistical variation decreases as the sample size increases. We note, from Fig. 11b, that the PDF peak also shifts from right to left as the size increases, confirming the size effect on the yield strength of the micro-pillars.

3.2. Applying the probability model to data from the thin film tests

The methodology which we used to deduct the model in Eq. (9) is also applicable to the data for the thin film tests. To make the model more inclusive and less loading specific, the we accounted for the data corresponding to the two different loading techniques: specifically the loading conditions are the uniaxial tensions with free boundaries and with symmetric boundaries. The yield stress for the thin films, corresponding to a 0.05% offset, is plotted in Fig. 12. The experimental data for microbulge tests on Cu free standing films and uniaxial tension tests on Cu with deformable substrates is also shown. We show that the majority of the experimental data mostly agrees with the trends predicted by the MDDP simulations. However, the MDDP simulations overestimate the strength of the films below the thickness 150 nm. This discrepancy may be attributed to the nucleation of dislocation dominating the plastic deformation at this range of thickness, and nucleation is not captured in our MDDP simulations (Akarapu et al., 2010). For thickness of 800 nm and larger, our simulations slightly underestimate the thin films strength. Generally this difference is due to the change in grain sizes. As mentioned previously, the strength is a function of both the grain size and the film thickness (Hommel and Kraft, 2001; Nix, 1989; Lawrence et al., 2012). The thin films we considered in this work are single crystals, likely to have a much flatter shape compared to the grains present in the experimental samples. Also in Fig. 12 the yield strength for thickness 2400 nm obviously deviates

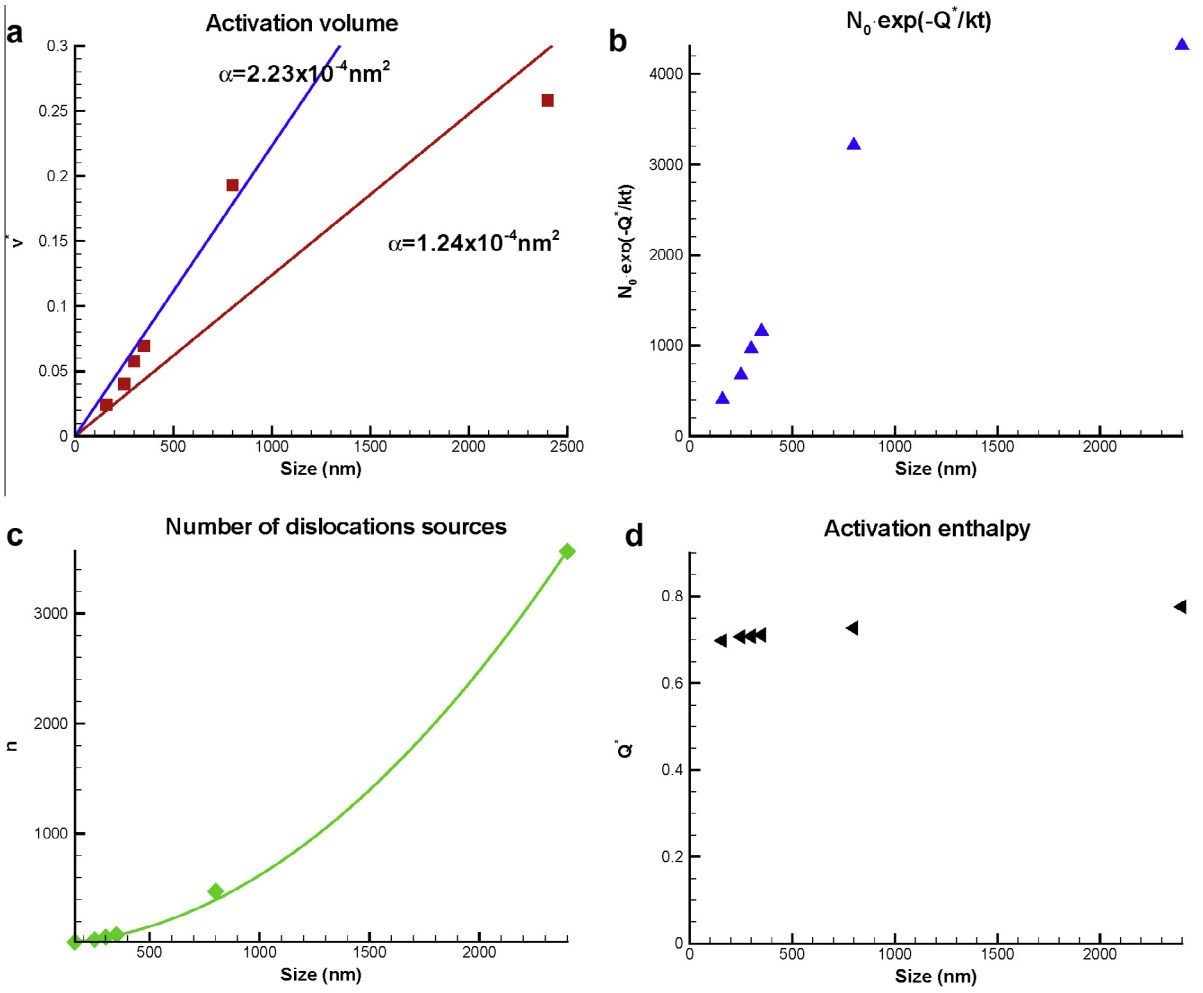

Fig. 13. The plots of (a) activation volume, (b) N_o .exp $(-Q^*/kt)$, (c) nominal number of sources, and (d) activation enthalpy with respect to the change of size (diameter) for the thin films.

Table 2
Fitting parameters for micro-pillars and thin films, the number in parenthesis takes the data point for thickness 2400 nm into account.

Parameters	α (nm^2)	β	Q^* (eV)
Micro-pillars	1.14×10^{-4}	10.95	0.72
Thin films	2.23×10^{-4} (1.24×10^{-4})	62	0.72

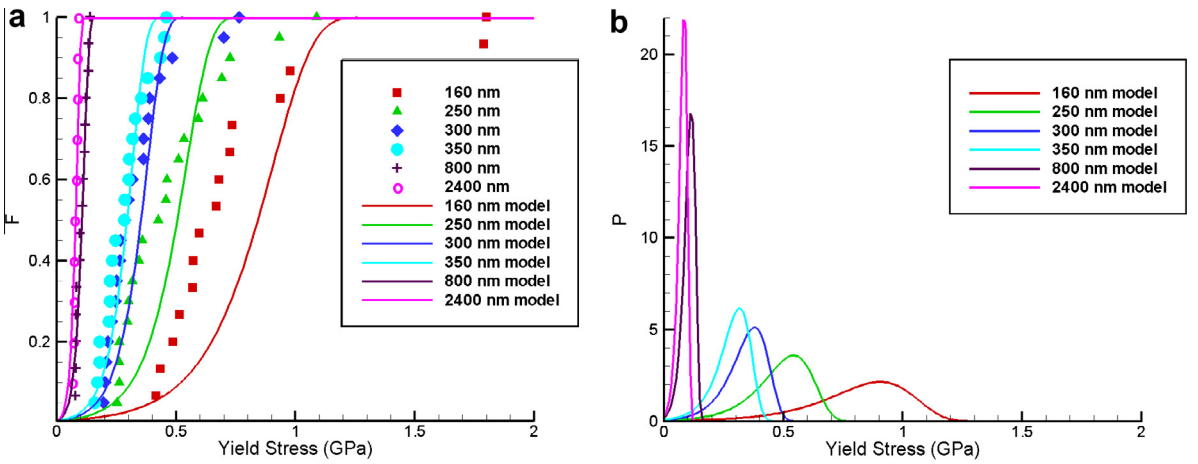

Fig. 14. The (a) fitted cumulative fraction curves and (b) resulting probability density functions for the thin films.

greatly from the power law predictions (red lines) compared to the rest of the data. This deviation is the consequence of the change in aspect ratio from $1 \times 5 \times 10$ to $1 \times 5 \times 5$ from thickness 800 nm to 2400 nm, resulting in a "thicker" grain. Hence, in the later analyses, this issue must be carefully addressed. Compared to the data of the micro-pillars (Fig. 7), the extent of the statistical variation is considerably smaller, even when the two different loading techniques are been considered. Similar to the micro-pillars observations, for thin films the amount of data spread decreases with increasing size (thickness in this case). This trend is true for both for the collection of all the data and for individual cases within each dislocation density and loading type group. Nonetheless, the numerical result shown in Fig. 12 can be fitted to a power law (Eq. (1)) with $n = 0.73$ comparable to the values calculated for the micro-pillars (Fig. 7).

Following the procedure performed in Section 3.1, the cumulative fraction plots are generated and then fitted using Eq. (7). The fitting results are shown in Fig. 13a–d. As expected the data points corresponding to thickness 2400 nm in υ^* and $N_0 \cdot \exp(-Q^*/kt)$ plots clearly deviate from other data points. In Fig. 13a, excluding the last data point the fitting yields $\alpha = 2.23 \times 10^{-4}$ nm^2. Including that point, the fitting becomes $\alpha = 1.24 \times 10^{-4}$ nm^2. This change suggests that a non-linear model for the activation volume is perhaps more suitable. The β value in Fig. 13c is determined to be 62. Thus the activation enthalpy is calculated to be $Q^* = 0.72$ eV. We note that the activation enthalpy for the dislocation in the micro-pillars and the thin films are the same. The fitting parameters for the micro-pillars and thin films are compared in Table 2.

The fitted cumulated fraction data and the resulting PDFs are shown in Fig. 14. The observation we made in the previous section is also valid within these graphs. First, the fitting of 160 nm cumulative fraction curve is poor compared to other curves. Also, the PDFs show a clear change in the width, height and position of the peaks corresponding to changes in the thin film thickness. This observation is consistent with the observations made in the case of the micro-pillars.

4. Conclusion

In this work we investigate the heterogeneous deformation behavior of micro-pillar compression, thin film microtensile and microbulge tests using multi-scale discrete dislocation simulations (MDDP), we focus on the statistical variation in the flow stress resulting from specimen geometry size and initial dislocation source heterogeneity. The size effect on strength, in the small volumes simulated here, is evident in both the mean strength values and the statistical variation of the data. We show the percent uncertainty of the yield strength decreases as a power law with the increase of the length scale through uncertainty analysis. Additionally our results suggest, for metallic structures in small volumes, the flow stress is stochastic and is dependent on the initial dislocation density and spatial distribution. This stochastic flow stress is a contrast to the traditional plasticity models, in which the yield stress is often treated as deterministic. The results indicate greater flow stress statistical variation in the micro-pillar simulation results than in the thin film microtensile simulations. This difference in statistical variation spread can be attributed to the interaction of dislocations with surfaces and stress concentrations.

The traction free boundary conditions and initial dislocation densities are consistent across both simulations; however, for the same dimensions, the thin film geometry has a larger surface area than the micro-pillar geometry. The consequence of these differing surface areas is that dislocations have a larger distance to sweep within the thin film. Within the micro-pillar case the main deformation mechanism is spiral motion of dislocations, but in the thin films the primary deformation mechanism is threading motion of the dislocations laid across the film thickness. The spiral mechanism tends to "contain" the deformation in a small region, producing strain bursts, and therefore the strength is very sensitive to the initial distribution of dislocations. As a result of this sensitivity a set of strength data, corresponding to a single micro-pillar size, may have a relatively large standard variation. In contrast, the mechanism of threading motion of dislocations, observed in thin films tends to distribute the deformation in a wider area; therefore, the strength in thin films is less sensitive to the initial dislocation density.

Based on these results a stochastic model of yield stress in micro- and nano-scale structures is developed through the use of nucleation theory. We suggest that the flow stress should be determined through a combination of scale size effects and probability analysis in future applications, such as plasticity models, and the comparison of experimental and atomistic simulation data. The determination of the yield stress should not be made solely through comparison with a threshold value. Instead the yield stress should be treated as a stochastic variable, in parallel with any traditional deterministic plasticity simulations, which can be quantified by Monte Carlo type simulations. This treatment stress will produce a stochastic yield stress based on the probabilistic distribution of finding and activating dislocation sources in a given small volume.

Acknowledgements

We gratefully acknowledge the support from NSF to WSU under Grant number CMMI 1030843.

References

Akarapu, S., Zbib, H.M., Bahr, D.F., 2010. Analysis of heterogeneous deformation and dislocation dynamics in single crystal micro-pillars under compression. Inter. J. Plast. 26, 239–257.
Benzerga, A.A., Shaver, N.F., 2006. Size dependence of mechanical properties of single crystals under uniform deformation. Scripts Mater. 54, 1937.
Brotzen, F.R., 1994. Mechanical testing of thin-films. Inter. Mater. Rev. 39, 24–45.
Dimiduk, D.M., Uchic, M.D., Parthasarathy, T.A., 2005. Size-affected single-slip behavior of pure nickel microcrystals. Acta Mater. 53, 4065–4077.
Deshpande, V.S., Needleman, A., Van der Giessen, E., 2005. Plasticity size effects in tension and compression of single crystals. J. Mech. Phys. Solids 53, 2661.
El-Awady, J.A., Biner, S.B., Ghoniem, N., 2008. A self-consistent boundary element, parametric dislocation dynamics formulation of plastic flow in finite volumes. J. Mech. Phys. Solids 56, 2019–2035.
El-Awady, J.A., Wen, M., Ghoniem, N.M., 2009. The role of the weakest-link mechanism in controlling the plasticity of micro-pillars. J. Mech. Phys. Solids 57, 32–50.
El-Awady, J.A., Rao, S.I., Woodward, C., Dimiduk, D.M., Uchic, M.D., 2011. Trapping and escape of dislocations in micro-crystals with external and internal barriers. Int. J. Plast 27, 372–387.
El-Awady, A.J., Uchic, M., Shade, P.A., Kim, S.-L., Rao, S., Dimiduk, D.M., Woodward, C., 2013. Pre-straining effects on power-law scaling of the size-dependent strengthening in Ni single crystals. Scripta Mater. 68, 207–210.
Espinosa, H.D., Panico, M., Berbenni, S.M., Schwartz, K.W., 2006. Discrete dislocation dynamics simulations to interpret plasticity size and surface effects in freestanding FCC thin films. Int. J. Plast 22, 2091–2117.
Fleck, N.A., Muller, G.M., Ashby, M.F., Hutchinson, J.W., 1994. Strain gradient plasticity–theory and experiment. Acta Metall. Mater. 42, 475.
Frick, C.P., Clarl, B.G., Orso, S., Schneider, A.S., Artaz, E., 2008. Size effect on strength and strain hardening of small-scale [111] nickel compression pillars. Mater. Sci. Eng., A 489, 319–329.
Fivel, M.C., Gosling, T.J., Canova, G.R., 1996. Implementing image stresses in a 3D dislocation simulation. Modell. Simul. Mater. Sci. Eng. 4, 581–596.
Gao, Y., Zhuang, Z., Liu, Z.L., Zhao, X.C., Zhang, Z.H., 2010. Characteristic Sizes for exhaustion-hardening mechanism of compressed Cu single-crystal micro-pillars. Chin. Phys. Lett. 27, 086103.
Gianola, D.S., Eberl, C., 2009. Micro- and nanoscale tensile testing of materials. J. Mine. Metal. Mater. Soc. 61, 24.
Groh, S., Marin, E.B., Horstemeyer, M.F., Zbib, H.M., 2009. Multiscale modeling of plasticity in aluminum single crystal. Int. J. Plast 25, 1456–1473.
Groh, S., Zbib, H.M., 2009. Advances in discrete dislocations dynamics and multiscale modeling. J. Eng. Mater. Tech. 131, 041209-1.
Gruber, P.A., Bohm, J., Onuseit, F., Wanner, A., Spolenak, R., Arzt, E., 2008. Size effects on yield strength and strain hardening for ultra-thin Cu films with and without passivation: a study by synchrotron and bulge test techniques. Acta Mater. 56, 2235–2318.
Guruprasad, P.J., Benzerga, A.A., 2008. Size effects under homogeneous deformation of single crystals: a discrete dislocation analysis. J. Mech. Phys. Solids 56, 132–156.
Hiratani, M., Zbib, H.M., 2002. Stochastic dislocation dynamics for dislocation-defects interactions. A multiscale modeling approach. J. Eng. Mater. Tech. 124, 335–341.
Hiratani, M., Zbib, H.M., 2003. On Dislocation-Defect Interactions and patterning: Stochastic discrete dislocation dynamics (SDD). J. Nuc. Materials 323 (2–3), 290–303.
Hommel, M., Kraft, O., 2001. Deformation behavior of thin copper films on deformable substrates. Acta Mater. 49, 3935–3947.
Huang, H., Spaepen, F., 2000. Tensile testing of free-standing Cu, Ag and Al thin films and Ag/Cu multilayers. Acta Mater. 48, 3261–3269.
Jaeger, G., Menzel, S., Schaper, M.K., 2006. A method of determining the strength of ductile thin films. Thin Solid Films 515, 2268–2273.
Khraishi, T., Zbib, H.M., 2002. "Free-surface effects in 3D dislocation dynamics: formulation and modeling," ASME. J. Eng. Mater. Technol. 124 (3), 342–351.
Kiener, D., Grosinger, W., Dehm, G., Pippan, R., 2008. A further step towards an understanding of size-dependent crystal plasticity: in situ tension experiments of miniaturized single-crystal copper samples. Acta Mater. 56, 580.
Kiener, D., Motz, C., Dehm, G., 2009. Micro-compression testing: a critical discussion of experimental constraints. Mater. Sci. Eng., A 505, 79–87.
Kobrinsky, M.J., Thompson, C.V., 2000. Activation volume for inelastic deformation in polycrystalline Ag thin films. Acta Mater. 48, 625.
Kraft, O., Gruber, P.A., Monig, R., Weygand, D., 2010. Plasticity in confined dimensions. Annu. Rev. Mater. Res. 40, 293–317.
Kubin, L., Canova, G., Condat, M., Devincre, B., Pontikis, V., Brechet, Y., 1992. Dislocation structures and plastic flow: a 3d simulation. Solid State Phenom. 23–24, 455–472.
Lawrence, S.K., Bahr, D.F., Zbib, H.M., 2012. Crystallographic orientation and indenter radius effects on the onset of plasticity during nanoindentation. J. Mater. Res. 27, 3058–3065.
Li, T.L., Bei, H., Morris, J.R., George, E.P., Gao, Y.F., 2012. Scale effects in convoluted thermal/spatial statistics of plasticity initiation in small stressed volumes during nanoindentation. Mater. Sci. Tech. 28, 1055.

Lee, S.W., Nix, W.D., 2012. Size dependence of the yield strength of fcc and bcc metallic micro-pillars with diameters of a few micrometers. Phil. Mag. 92, 1238–1260.
Ma, Q., Clarke, D.R., 1995. Size-dependent hardness of silver single crystals. J. Mater. Res. 10, 853.
Mason, J.K., Lund, A.C., Schuh, C.A., 2006. Determining the activation energy and volume for the onset of plasticity during nanoindentation. Phys. Rev. B 72, 054102.
Martinez, R., Ghoniem, N.M., 2002. The influence of crystal surfaces on dislocation interactions in mesoscopic plasticity: a combined dislocation dynamics-finite element approach. Comput. Model. Eng. Sci. 3, 229–243.
Nix, W.D., 1989. Mechanical properties of thin films. Metall. Trans. A 20A, 2217.
Nix, W.F.D., Gao, H., 1998. Indentation size effects in crystalline materials: a law for strain gradient plasticity. J. Mech. Phys. Solids 46, 411.
Ng, K.S., Ngan, A.H.W., 2008a. Breakdown of Schmid's law in micro-pillars. Scri. Mater. 59, 796–799.
Ng, K.S., Ngan, A.H.W., 2008b. A Monte Carlo model for the intermittent plasticity of micro-pillars. Model. Simul. Mater. Sci. Eng. 16, 055004.
Ng, K.S., Ngan, A.H.W., 2008c. Stochastic theory for kerky deformation in small crystal volumes with pre-existing dislocations. Phil. Mag. 88, 677–688.
Ngan, A.H.W., Ng, K.S., 2010. Transion from deterministic to stochastic deformation. Phil. Mah. 90, 1937–1954.
Rao, S.I., Dimiduk, D.M., Parthasarathy, T.A., Uchic, M.D., Tang, M., Woodward, C., 2008. A thermal mechanisms of size-dependent crystal flow gleaned from three-dimensional discrete dislocation simulations. Acta Mater. 56, 3245–3259.
Rhee, M., Hirth, J.P., Zbib, H.M., 1994. A superdislocation model for the strengthening of metal-matrix composites and the initiation and propagation of shear bands. Acta Metall.Mater. 42, 2645–2655.
Rhee, M., Zbib, H.M., Hirth, J.P., Huang, H., Diaz de la Rubia, T., 1998. Models for long-/short-range interaction and cross slip in 3D dislocation simulation of BCC single crystals. Modell. Sim. Mater. Sci. 6, 467–492.
Rinaldi, A., Peralta, P., Sieradzki, K., Traversa, E., Licoccia, S., 2012. Role of dislocation density on the sample-size effect in nanoscale plastic yielding. J. Nanomech. Micromech. 2, 42–48.
Schneider, A.S., Frick, C.P., Clark, B.G., Gruber, P.A., Arzt, E., 2011. Influence of orientation on the size effect in bcc pillars with different critical temperatures. Mater. Sci. Eng., A 528, 1540–1547.
Schneider, A.S., Kiener, D., Yakacki, C.m., Maier, H.J., Gruber, P.A., Tamura, N., Kunz, M., Minor, A.M., Frick, C.P., 2013. Influence of bulk pre-straining on the size effect in nickel compression pillars. Mater. Sci. Eng., A 559, 147–158.
Schuh, C.A., Lund, A.C., 2004. Application of nucleation theory to the rate dependence of incipient plasticity during nanoindentation. J. Mater. Res. 19, 2152.
Shan, Z.N., Mishra, R.K., Syed-Asif, S.A., Warren, O.L., Minor, A.M., 2008. Mechanical annealing and source-limited deformation in submicrometre-diameter Ni crystals. Nature 7, 115.
Shehadeh, M., Bringa, E.M., Zbib, H.M., McNaney, J.M., Remington, B.A., 2006. Simulation of shock-induced plasticity including homogeneous and heterogeneous dislocation nucleations. App. Phys. Lett. 89, 171918.
Stolken, J.S., Evans, A.G., 1998. A microbend test method for measuring the plasticity length scale. Acta Mater. 46, 5109.
Tang, H., Schwarz, K.W., Espinosa, H.D., 2007. Dislocation escape-related size effects in single-crystal micro-pillars under uniaxial compression. Acta Mater. 55, 1607–1616.
Tang, H., Schwartz, K.W., Espinosa, H.D., 2008. Dislocation-source shutdown and the plastic behavior of single-crystal micro-pillars. Phys. Rev. Lett. 100, 185503.
Van der Giessen, E., Needleman, A., 1995. Discrete dislocation plasticity: a simple planar model. Model. Simul. Mater. Sci. Eng. 3, 689–735.
Uchic, M.D., Dimiduk, D.M., Florando, J.N., Nix, W.D., 2004. Sample dimensions influence strength and crystal plasticity . Science 305, 986.
Xiang, Y., Tsui, T.Y., Vlassak, J.J., 2006. The mechanical properties of freestanding electroplated Cu thin films. J. Mater. Res. 21, 1607.
Yasin, H., Zbib, H.M., Khaleel, M.A., 2001. Size and boundary effects in discrete dislocation dynamics: coupling with continuum finite element. A Mater. Sci. Eng. 309–310, 294–299.
Yu, D.Y.W., Spaepen, F., 2004. The yield strength of thin copper films on Kapton. J. App. Phys. 95, 2991.
Zaiser, M., Schwerdtfeger, J., Schneider, A.S., Frick, C.P., 2010. Strain burts in plastically deforming molybdenum micor- and nanopillars. Phil. Mag. 88, 3861–3874.
Zbib, H.M., Rhee, M., Hirth, J.P., 1998. On plastic deformation and the dynamcis of 3D dislocations. Int. J. of Mech. Sci. 40, 113–127.
Zbib, H.M., de la Rubia, T.D., 2002. A multiscale model of plasticity. Inter. J. Plast. 18, 1133–1163.
Zbib, H.M., and Akarapu, S., 2009. Modeling of plasticity and deformation mechanisms in sub-micrometer size crystalline materials. *Proceedings of the 2nd International Symposium on Steel Science, Kyoto,* Japan.
Zbib, H.M., Overman, C., Akasheh, F., Bahr, D.F., 2011. Analysis of plastic deformation in nanoscale metallic multilayers with coherent and incoherent interfaces. Int. J. Plasticity 27, 1618–1638.
Zhang, X., Aifantis, K.E., 2011. Interpreting strain bursts and size effects in micro-pillars using gradient plasticity. Mat. Sci. Engg. A 528, 5036.
Zhou, C., Biner, S.B., LeSar, R., 2010. Discrete dislocation dynamics simulations of plasticity at small scales. Acta Mater. 58, 1565–1577.
Zhu, T., Li, J., Samanta, A., Leach, A., Gall, K., 2008. Temperature and strain-rate dependence of surface dislocation nucleation. Phys. Rev. Lett. 100, 025502.